Nanometer Scale Science and Technology - The impact of STM and AFM

M. Hegner and H.-J. Güntherodt

Department of Physics and Astronomy; National Center of Competence in Research (NCCR) on Nanoscale Science, Klingelbergstr. 82, University of Basel, CH-4056 Basel; Switzerland

1. – Introduction

The field of Nanometer Scale Science and Technology (NSST) is very broad, ranging from nanoparticles, nanoclusters, mesoscopic systems and nanoconstrictions, to individual atoms and molecules and their self-assembly into defined structures such as nanowires or biomolecules. This is a field where the border between the traditional disciplines like physics, chemistry and biology is no longer detectable and interesting synergies arise, e.g., instruments developed in physics provide the precision and sensitivity to perform specific molecular recognition experiments in biology.

1˙1. *Relation of NSST and SPM*. – Scanning Probe Methods (SPM) such as Scanning Tunnelling Microscopy (STM), Atomic Force Microscopy (AFM) and Scanning Nearfield Optical Microscopy (SNOM) (see the lecture on this topic this volume) have a strong impact on NSST. SPM are the eyes (microscopes) and tools of NSST, as has been shown convincingly by imaging, spectroscopy, modification and manipulation. Of particular interest are the cantilever based AFM related Nano-Electro-Mechanical Systems (NEMS) opening the doors of nanomechanics to a new world. Nowadays we have the chance to study the development of collective properties of condensed matter from single atoms, to measure individual bonds between two atoms, to detect changes in stress, heat and mass towards the ultimate limits and to sense physical, chemical and biological properties at a previously unknown level. We are able to correlate thermodynamic ensemble averages to properties measured on single atoms and molecules. SPM will elucidate the

high resolution end of NSST, the world of atoms and molecules and SPM will therefore contribute to unprecedented understanding and control over the fundamental building blocks of condensed matter.

1˙2. *The roots of NSST.* – The roots of NSST go back to Feynman [1], the originator of the famous sentence "There is plenty of room at the bottom". His focus was on tools based mainly on electron microscopes. Taniguchi [2] contributed to the roots by stressing the importance of the nanometer in precision mechanics.

The breakthrough occurred with new types of microscopes (SPM), materials (carbon-based fullerenes, nanotubes and quantum dots), mesoscopic systems, new trends in miniaturization based on the view of chemists and the vision that nature is the best example of nanotechnology.

In this discussion it is of interest to know the answers to the questionnaire:

- Significant SCIENTIFIC discoveries
- Significant TECHNOLOGICAL advancements

at the workshop "Vision of Nanotechnology R+D in the Next Decade" [3] organized on behalf of the Interagency Working Group on Nano-Science, Engineering and Technology (IWGN).

The quoted significant scientific discoveries are

- the development of SPM and atom manipulation;
- the discovery of fullerenes, nanotubes, nanocrystals and quantum dots;
- demonstration of single electron devices at room temperature;
- demonstration of molecular electronic devices;
- biological examples of functional nanostructures: rotary motors, self/non-self recognition.

The quoted significant technological advancements are

- expansion of types and uses of SPM;
- nano-lithography via molding and stamping as low-cost, high-throughput nanopatterning technologies with sub 10 nm feature size;
- Micro-Electro-Mechanical Systems (MEMS) or Nano-Electro-Mechanical Systems (NEMS);
- high-speed AFM-based lithography.

It becomes obvious how important SPM already is for NSST and that it will become even more in the future.

1˙3. *The background of STM, AFM: SPM*. – It was a long way to go from Frenkels [4] theory relating the electrical current and the exponential dependence of the distance d in vacuum tunnelling to the most elegant scanning tunnelling microscope by Binnig, Rohrer and collaborators [5].

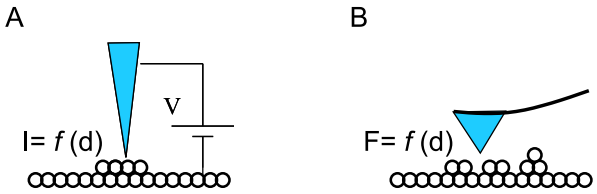

Figure 1. – (A) Scheme of a STM, feedback signal is the current (I) (B) Scheme of an AFM, feedback signal is the force (F).

At the time STM was invented, research in tunnelling focused on planar oxide junctions, to determine the superconducting energy gap [6] or to study the inelastic electron tunnelling spectroscopy (IETS) and their relation to IR spectroscopy [7]. Also spin-polarized tunnelling of electrons through oxide barriers was a topic. All these experiments with oxide barriers called for similar experiments by vacuum barriers. Very soon the extension to other tip sample interactions (light, forces etc.) became obvious and in 1984 Pohl et al. [8] invented the SNOM. The pioneering development of the AFM by Binnig, Quate and Gerber [9] opened up an even larger field. Figure 1 shows the schematic setup of an STM (A) and an AFM (B), respectively.
The impact today and the possible future influence of SPM, in particularly AFM (our major research topic), on NSST will be highlighted in the following chapters.

2. – Highlights of STM studies

2˙1. *Imaging*. – The first achievement of STM was the very impressive image of the Si(111)7×7 structure at the IBM Research Laboratory Rüschlikon [10]. Figures 2 A

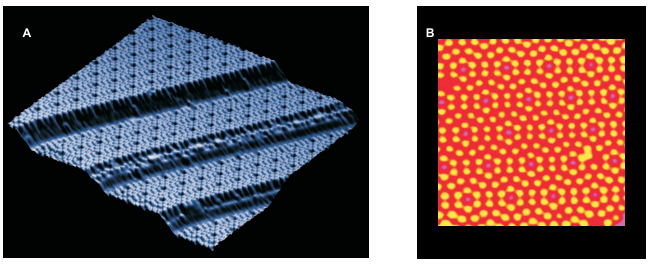

Figure 2. – Si(111)7×7 surface measured by STM [11].

and B show examples of such images obtained on a Si(111)7×7 surface in the presence

of multiple-step edges [11]. Figure 2 A shows an overview with three steps between reconstructed terraces. Figure 2 B shows an image on one terrace. From the Rüschlikon Laboratory the STM method has spread all over the world. Later followed images on other semiconductors, metals and organic molecules absorbed on surfaces. For recent results in the last field, see the review of Hamers in this volume [12].

Today, STM is an important part of surface science. The field is summarized in the Proceedings of the International STM Conferences and by several reviews. In addition to imaging, the field is becoming important for NSST in other ways as illustrated by the experiments summarized in the following sections.

2˙2. *Modification.* – In 1985, it became clear that STM, in addition to an imaging device, can also be used to modify surfaces. The first demonstration of this was a lithographic nanometer line pattern on an atomically flat surface of a metallic glass [13]. There is also the possibility of direct writing of nanometer scale structures by making Taylor cones on metallic glasses with enhanced local current density and strong electric field [14, 15]. More recently the field of STM lithography has become important.

2˙3. *Atom manipulation.* – The next step was the pioneering work of Don Eigler and his collaborators to manipulate atoms at low temperature [16]. Several of these scientists

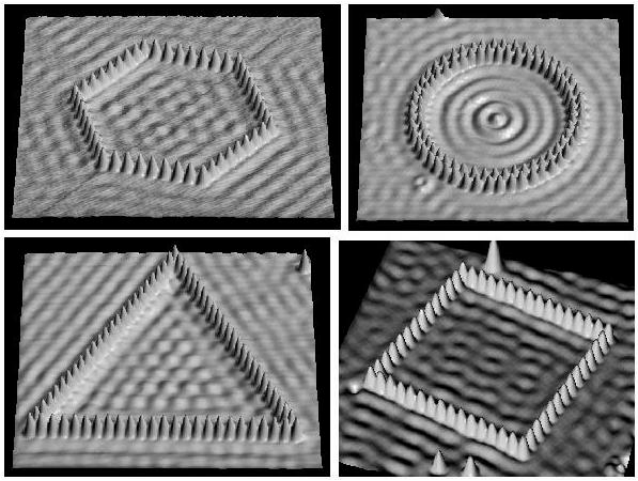

Figure 3. – Electron waves on a metal surface and quantum corrals: Iron on Copper (111) [16]

made model structures, as shown in Fig. 3. These type of experiments demonstrated the first atomic scale device, the atomic switch. Later, researchers at Hitachi suggested the atom relay transistor. A very recent highlight is the quantum mirage [17]. The field of manipulation of molecules at room temperature has been developed by Jim Gimzweski and his collaborators [18]. For an overview see [19, 20]. A very surprising result was the room temperature manipulation of Bromine on surfaces [21]. This is an other example

demonstrating how rich the field of new discoveries is.

2˙4. *Studies of superconductors.* – The next highlight in STM was the application to superconductors, to measure the spatial distribution of the BCS energy gap and to image the vortex lattice in the type-II superconductor $NbSe_2$ [22]. Later, the vortex pinning by columnar defects in a $NbSe_2$ crystal was studied by STM [23]. The vortex arrangement can be directly compared to the defect distribution. Additional highlights are: the observation of the tunnelling of Cooper pairs (Josephson tunnelling) through a vacuum barrier instead of an oxide barrier [24]. The contributions of s- and d-waves to superconductivity in high-temperature superconductors in the mK-range [25].

2˙5. *Inelastic electron tunnelling spectroscopy.* – At the end of the nineties the long awaited success in inelastic electron tunnelling spectroscopy by STM occurred [see e.g. [26]]. As a consequence, the field of single-molecule vibrational spectroscopy and microscopy has developed as a powerful tool for the analysis of molecules absorbed on surfaces. Inelastic electron tunnelling spectra for an isolated acetylene (C_2H_2) molecule absorbed on the Cu (100) surface showed an increase in the tunnelling conductance at 358 millivolts, resulting from excitation of the C-H stretch mode. An isotropic shift of 266 millivolts was observed for deuterated acetylene (C_2D_2).

3. – Introduction to AFM: contact mode

3˙1. *Imaging.* – The development of the AFM gives an alternative to STM. STM senses the surface topography *via* tunnelling current and is applied on conducting sample surfaces. The AFM measures the topography by detecting the forces between the tip

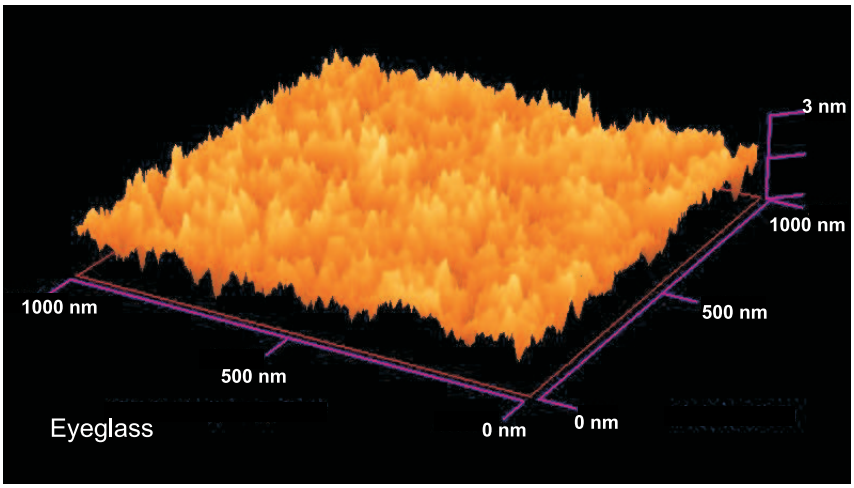

Figure 4. – Highly polished glass surface of an eye glass

and the sample, an alternative name is Scanning Force Microscope (SFM). It can be applied to any surface but has proved to be a great tool on insulating surfaces and is easy to apply in physiological environments to investigate biological samples. It has also the potential of measuring small forces on a local scale.

The force interaction between tip and sample can be studied in the contact or non-contact, static or dynamic modes. The breakthrough in the field was obtained by using microfabricated cantilevers, which led to reproducible images.

AFM became very popular because it can be used to image everyday life and industrial samples beyond the resolution of the state-of-the-art optical microscopes. Figure 4 shows the topography of an optical polished eye glass which compares to the panorama of the Swiss Alps with valleys and mountains.

Today, the testing of many modern hightech products such as CDs, ICs, magnetic

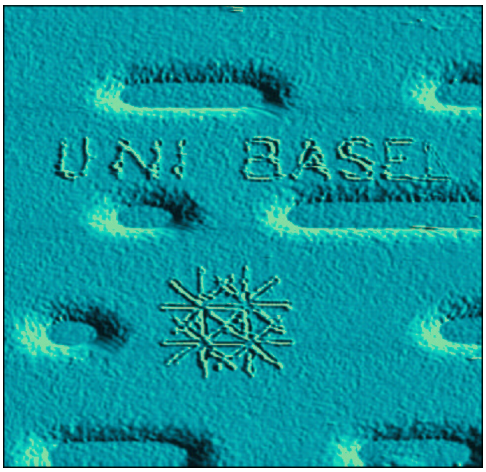

Figure 5. – Modified CD surface by SFM.

storage media and heads etc. is a broad field for applications of commercial SFMs. The SFM can also be applied to modify surfaces. Figure 5 shows the writing on a polymeric surface using a cantilever under larger forces than applied for imaging. In ambient conditions the samples are covered by a water layer which makes the interactions more complex. There is a crucial problem with atomic resolution in the contact mode. It is possible to see atomic periodicity, but not the detailed atomic structures, in particular no defects or vacancies. However, great progress has been mad by imaging biological samples [27], [28]

In addition to the field of imaging with the AFM two other applications developed.

3˙2. *Friction Force Microscopy (FFM).* – The friction force microscope [29], [30] provided the chance to produce a single asperity contact and study friction on the atomic scale. Figure 6 shows the scheme of an FFM. In an FFM, a flat surface is scanned by a

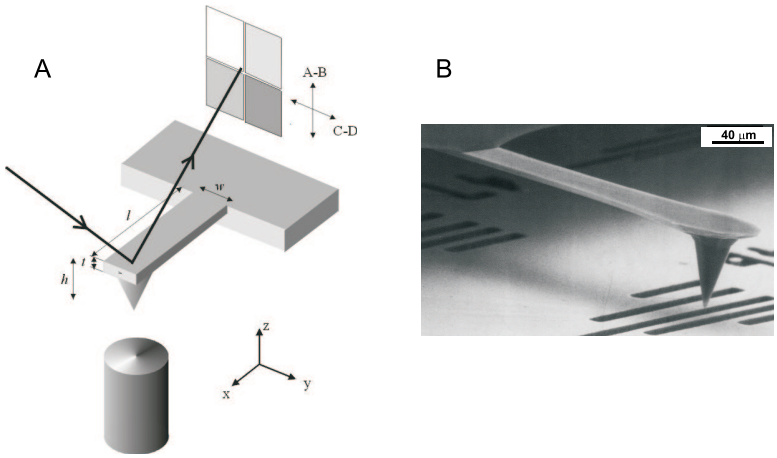

Figure 6. – (A) Scheme of an FFM instrument. By recording the torsion signal of the cantilever (C↔D) a frictional force can be correlated. (B) SEM picture of a Si cantilever.

sharp tip at a constant normal force or height; the lateral (or friction) force is detected by optical techniques which measure the torsional bending of the cantilever where the tip is mounted. By FFM measurements it was revealed that friction laws for a single

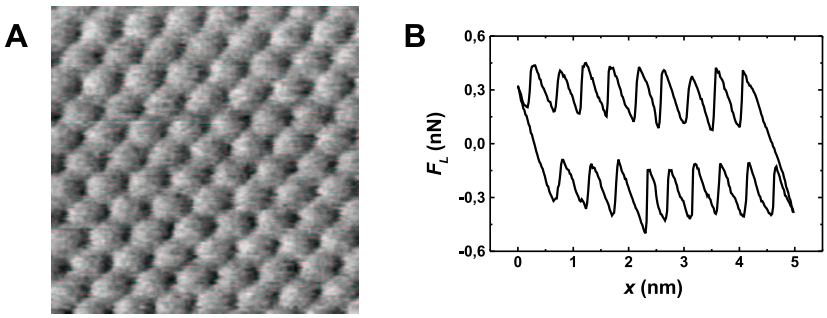

Figure 7. – A) Lateral force image of NaCl. B) Slick-slip hysteresis of forward and backward scan line.

asperity are different from macroscopic friction laws. The main result, confirmed by several experiments, is that the friction on the nanometer scale exhibits a sawtooth behavior, commonly known as atomic stick-slip. This phenomenon can be theoretically reproduced within classical mechanical models. Figure 7 shows A) the lateral force map of NaCl (100) at an applied force F_N= 0.65 nN and scan velocity v= 25 nm/s, B) the friction loop formed by a forward and backward scan line, respectively. In this experi-

ment [31], a silicon tip has been used and a velocity dependence of atomic-scale friction has been discovered.

3˙3. *Molecular recognition experiments.* – A fundamental prerequisite for the amazing complexity of life is specific recognition at the molecular level. The interplay of multiple non-covalent bonds (e.g. electrostatic, electrodynamic (van der Waals), or hydrogen) or hydrophobic interactions is the basis for highly specific interactions. The direct measurement of intermolecular interactions under physiological conditions becomes feasible by AFM. Examples are published from biotin/streptavidin [32, 33], from complemen-

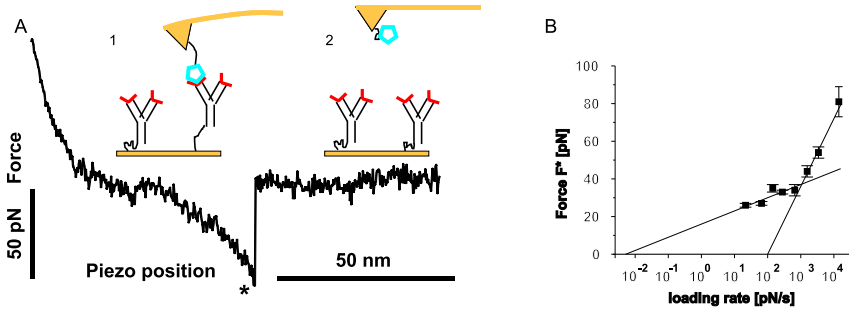

Figure 8. – (A) Biorecognition experiment. The tip is approached to the surface until contact occurs. A specific interaction takes place . (1) Retracting the cantilever stretches the linker which connects the single biomolecules covalently to the surfaces. When the force reaches the unbinding force of the complex, the biological interaction is ruptured (*) and the cantilever is available for (2) a new force distance curve. (B) Loading rate dependence of the unbinding forces of the avidin-biotin system under physiological conditions [38].

tary DNA strands [34], adhesion proteoglycans [35], antigen/antibody [36], proteins, etc. Fig. 8 shows a schematic of the measuring principle for the antigen and antibody interaction. The antigen is immobilized on the tip and the antibody covers the sample surface. A typical retract force distance curve is shown in the lower part of Fig. 8A.

These experiments have developed the field of force-induced dissociation of a ligand-receptor bond. A comparison of these single event results with thermodynamic data (affinity) becomes possible by taking into account the loading rate for these experiments [37]. By plotting the dependence of the average unbinding force *versus* the retract velocity for a specifically interacting tip with a surface and extrapolating a linear fit to zero unbinding force gives an estimate for the thermal off-rate ν_0 of the biological complex (Fig. 8 part B). If intermediate binding states exist as in the example of biotin/avidin two regimes can be distinguished, which allow one to deduce the scaling factor Δx within the equation $\nu \approx \nu_0\, exp(F\Delta x/k_BT)$ from the slope of the fit. If multiple stable intermediate states exist, more than one slope can be fitted to the experimental data [37, 38].

4. – Noncontact AFM

4˙1. *Experiments.* – In 1995 Giessibl [39] was able to show rudimentary atomic resolution on the Si(111)7×7 surface using dynamic mode SFM operating in ultra-high vacuum (UHV). This opened the new field of true atomic resolution and allowed the observation of defects and vacancies. There was also a demonstration of true atomic resolution in water [40].

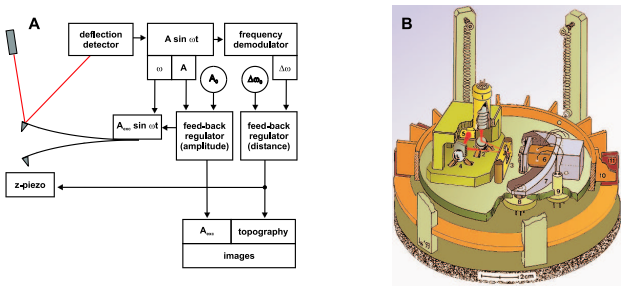

Figure 9. – (A) Schematic layout for the operation of a noncontact AFM. (B) Setup of a UHV Dynamic Force Microscope .

Figure 9 shows the setup of a noncontact UHV AFM instrument [41]. Imaging is performed in the dynamic mode using a frequency modulation (FM) technique in which the cantilever is driven at its resonance frequency. The first publication of Giessibl was followed by a period of reproducing his results and to obtain larger scan sizes [42]. The Si(111)7×7 surface was an excellent benchmark to compare STM and SFM experiments at room temperature and finally at low temperatures.

4˙2. *Room temperature results.* – Figure 10 shows tunnelling current and measured frequency shift measured while approaching the Si surfaces. The distance range near the

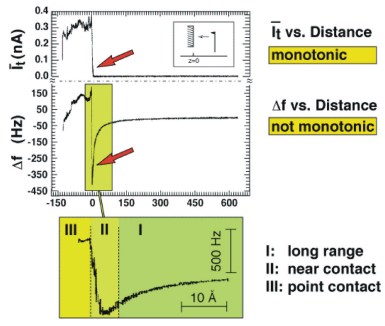

Figure 10. – Simultaneously recorded traces of the tunnelling current (time averaged) $\bar{I}_t$ (top) and frequency shift vs. distance (bottom) [42].

change from attractive to repulsive forces (decreasing to increasing frequency shift) was the most suitable to obtain true atomic resolution [43]. Simultaneous STM and SFM yields images by tunnelling current and forces and in addition so-called "dissipation" images (Fig. 11), which refers to the energy provided to obtain a constant oscillation

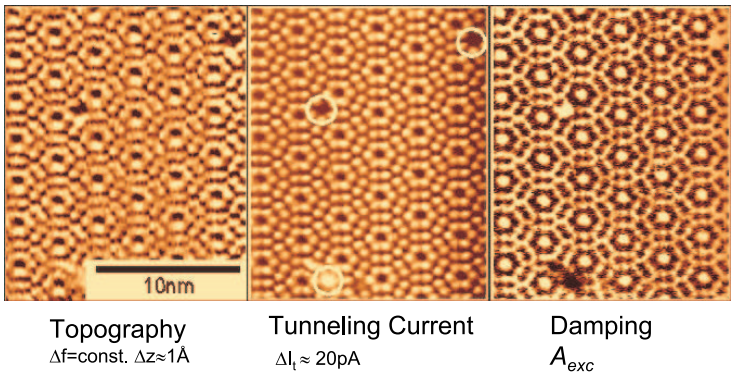

Figure 11. – Simultaneously recorded images of Si(111)7×7 at constant Δf [43].

amplitude of the dynamic cantilever [44]. The noncontact SFM is also able to give atomic resolution images on insulators. Figure 12 shows a layer of NaCl on Cu. Most

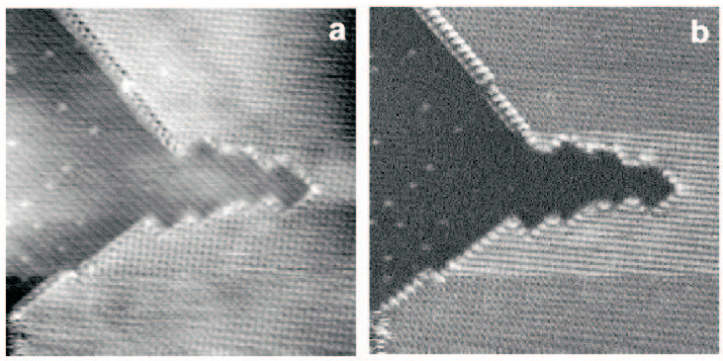

Figure 12. – NaCl island on Cu(111). Step atoms and kink and edge sites give different contrast. The image size is 18×18 nm^2 [44].

impressive is the contrast observed between atoms in the center of the layer and at the edge or kink sites due to the different interaction forces associated with these sites. Here one of the fundamentals of catalysis becomes very obvious, the high reactivity of the kink and edge sites.

4˙3. *Low temperature results.* – A low temperature SFM operating in a dynamic mode in ultra-high vacuum was used to study the Si(111)7×7 surface at 7.2 K. Not only the twelve adatoms but also the six rest atoms of the unit cell are clearly resolved. These images are of a quality comparable to STM. Figure 13 shows the corresponding image [45]. SFM operation at low temperatures reduces the thermal vibration in the cantilever resulting in improved sensitivity. In addition, thermal drift is significantly

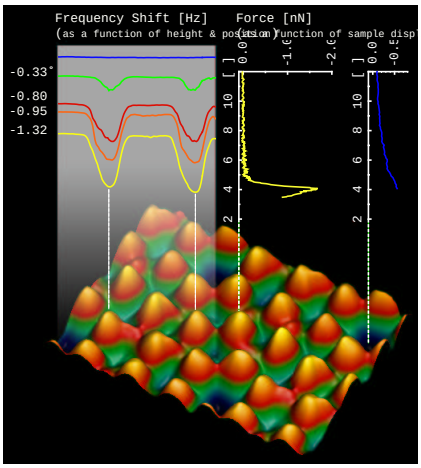

Figure 13. – Si(111)7×7 surface measured by AFM in UHV at low temperature (7.2 K). Line sections: Frequency shift measurements as a function of distance between tip and surface [45]

reduced allowing more accurate positioning and the use of slower scan speeds.

The performance of this instrument allows the direct measurement of short-range chemical bonding force acting between the foremost atom on the apex of a silicon AFM tip and specific atomic sites on a Si(111)7×7 sample. The resolution of the measurements was sufficient to distinguish differences in the interaction potentials between inequivalent adatoms, demonstrating the ability of AFM to provide quantitative, atomic scale information on surface chemical reactivity. These measurements provide insight into the nature of covalent bonding and have important implications for understanding the mechanisms responsible for contrast formation in true atomic resolution AFM. An accurate description of the short-range chemical forces which bind atoms together is of fundamental importance to our basic understanding of the properties of matter on both the nanoscale and on the macroscopic level.

4˙4. *Magnetic Force Microscopy.* – Magnetic Force Microscopy (MFM) has become a valuable tool for measuring the stray field of complex ferromagnetic samples and superconductors. The detection device consists of a micron-scale ferromagnetic tip attached to a flexible cantilever which scans close to the surface of the sample. The stray field emanating from the topography of the sample allows a correlation of the measured stray

field with significant surface structures. Therefore it is possible to study the pinning of domain walls in ferromagnetic samples and the pinning of vortices in superconducting samples due to structural defects seen at the surface. Other applications are the use of the stray field of the tip for modifying the magnetic state of the sample. Also MFM can be used for the determination of the sensitivity and response of magnetic heads and storage media to localized fields.

There is growing interest moving from qualitative imaging to quantitative analysis [46] of sample properties using MFM. In general it is not possible to calculate a magnetization distribution from MFM data. In the special case of perpendicular magnetization it is theoretically possible to use the force pattern, $F(x, y)$, to generate the magnetization pattern, $M(x, y)$, to within a constant. However due to the limited signal-to-noise ratio of a MFM force measurement the better procedure remains to assume a magnetization pattern, calculate its field and then calculate the force on the tip due to this field. This calculated force is then compared with the measured force data. This process is iterated

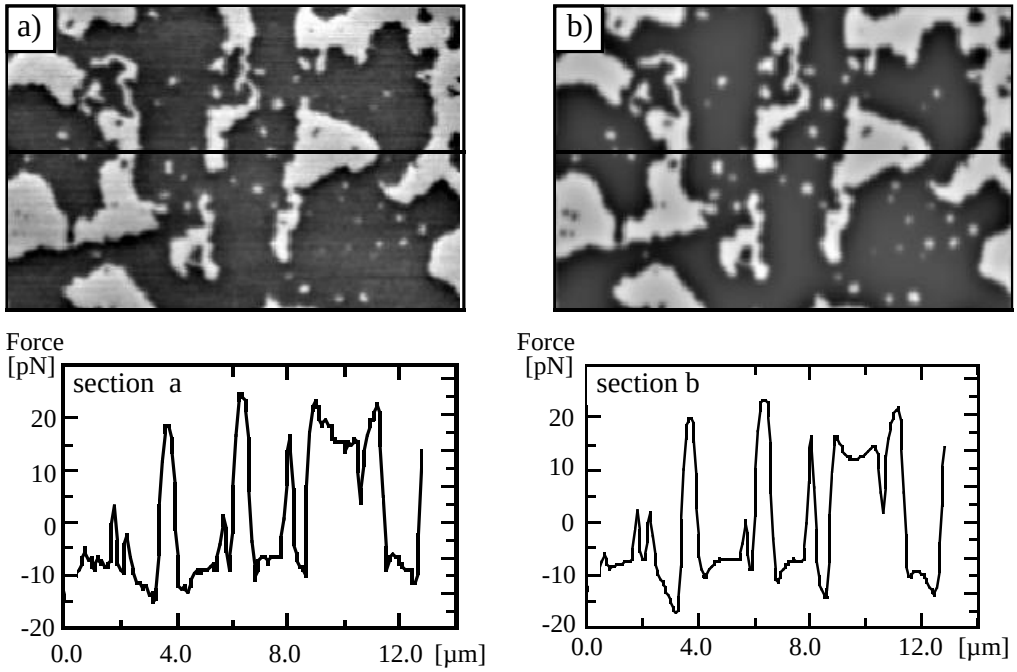

Figure 14. – Simulation of MFM data. (a) MFM measurement of a Cu/Ni(10 nm)/Cu/Si(001) thin film showing perpendicular magnetization. (b) The simulation of the MFM image is generated from the magnetization pattern using the transfer theory. (Section a, Section b) Cross section of the MFM measurement and the simulation [47].

until the agreement between measured and calculated force pattern is optimized.

For illustration purpose MFM examples on ferromagnetic and superconducting sam-

ples are shown. Figure 14 shows MFM measurements [47] on a 10 nm thick Ni film (sandwiched between Cu layers on Si(001)) with perpendicular magnetization (a) and the corresponding simulation of the MFM image (b). The bottom of the figure shows the cross-section of the measurements and simulations. Good agreement between experiment and simulation is obtained.

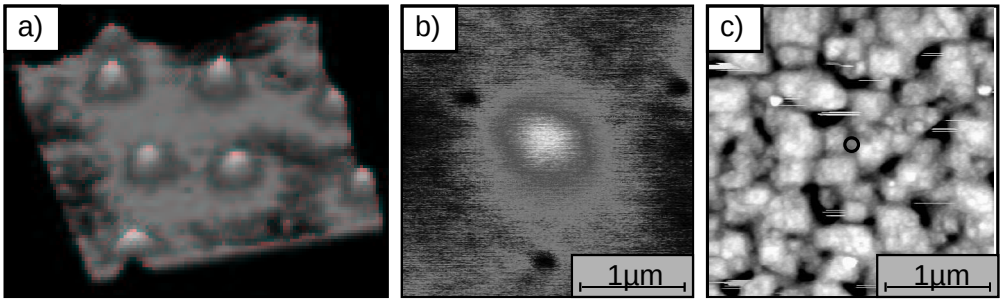

Figure 15. – In laser ablated $YBa_2Cu_3O_{7-\delta}$ (YBCO) thin films a non-crystalline arrangement of vortices is observed (a). The number of vortices imaged per unit area coincides well with that expected from the applied field. (b) shows the magnetic stray field of one single vortex. the stray field has to be compared to the corresponding topography image (c) [48].

Figure 15 shows a glass-like vortex arrangement in a laser-ablated YBCO thin film [48]. Such a glass-like vortex structure indicates that the vortex arrangement is dominated by the pinning force rather than by the repulsive inter-vortex forces. The number of single vortices imaged per unit area coincides well with that expected from the image area and the applied field. The topography of YBCO thin films is either dominated by screw dislocations or by tower-like islands. The vortices are always pinned between the islands and never in the center of screw dislocations or in the lowest locations.

Figure 16 shows vortex pinning in an YBCO single crystal which is related to twin boundaries [49]. Shown are vortices obtained in fields ranging from 0.5 to 6.4 mT. This field regime is comparable to that used in decoration experiments. There is a one-dimensional ordering of the vortices along the crystallographic [110] directions, which is the direction of twin-boundaries [49]. For a better comparison of the different measurements a topographical defect visible in the center of the image has been marked by a white circle. In addition we have overlayed the images with the same fixed set of white lines. A solid line represents the directions and the exact location of a chain of vortices. The vortices are always exactly centered on the line. In contrast, a dashed line represents a location where a chain of vortices appears at certain fields but is not fixed in space. A good example is the dashed line running approximately through the center of the images. In low fields (0.5 mT, 0.99 mT and 1.8 mT) no vortices are present on these line. In the slightly higher field of 3.6 mT, two vortices appear. One of them is centered nicely on the line, whereas the second one is clearly located beside the line. At 5.7 mT the dashed line marks a chain of vortices with a density only slightly below that of the two

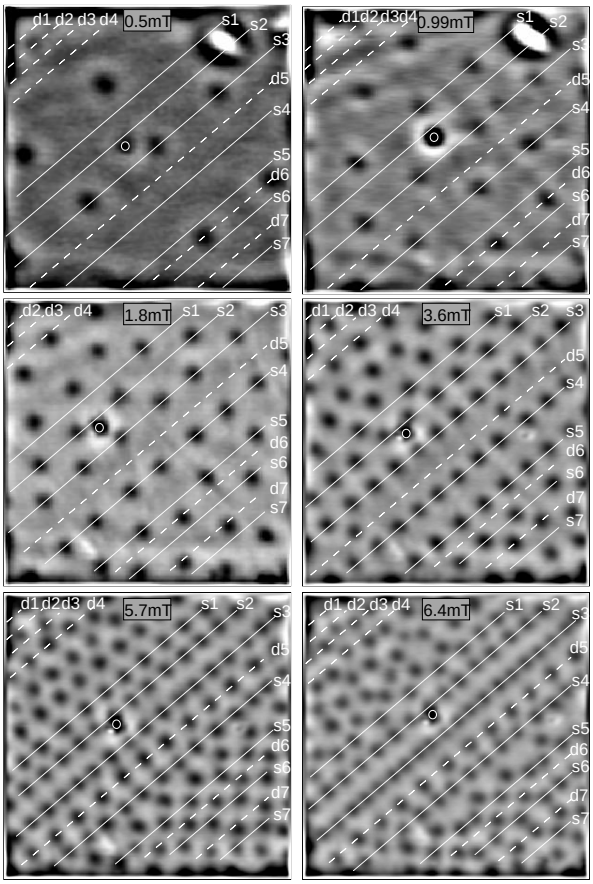

Figure 16. – Vortex arrangements at low fields (0.5 mT-8 mT) [49].

adjacent chains marked by solid lines. Note that the vortex chain marked by the dashed line is perfectly centered between the ones indicated by the two solid lines. Furthermore, the vortices on the dashed line are shifted in order to maximize the distances to those located on the solid lines. When the field is further increased to 6.4 mT the left of the two solid lines features a higher vortex density than the line on the right. The vortices indicated by dashed line are consequently located closer to the right line.

These observations suggest that the vortices on the solid lines are pinned at twin boundaries, whereas the vortices in the space between them may order if the inter-vortex distance given by the external field and the distance between the twins match certain geometrical conditions.

Other experimental techniques have been used to image vortices, e.g., Scanning SQUID Microscopy [50, 51] or Scanning Hall Probe Microscopy [52, 53]. However, the impact on NSST is mainly expected from MFM. The MFM will be improved by the demon-

strated atomic resolution with noncontact AFM and will move into the high-resolution regime where essential, still open, questions in nanomagnetism, magnetic nanoconstrictions, exchange force microscopy etc. can be addressed.

5. – AFM related experiments-Nanomechanics

5˙1. *Fundamentals*. – There are several characteristic features of cantilevers making AFM based devices very appropriate for use as a sensor for stress, heat and mass (see schematic in figure 17) capable of measuring quantities below the detection limits of equivalent "classical" methods and towards the ultimate limits of measurements. The

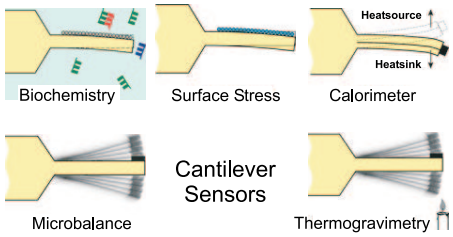

Figure 17. – Different types of cantilever sensors.

characteristic features of cantilevers are: fast responses, high sensitivity, high resonance frequencies, small excitation energies and suitable for mass production!

The field of cantilever based sensors started with the observation of the catalytic chemical reaction of H_2 and O_2 to water on a bimetallic microfabricated cantilever covered by a Pt surface [54]. Later on the surface stress in self assembled monolayers was measured directly [55].

5˙2. *Nanocalorimeter*. – In 1996 the first attempt for thermal analysis using a micromechanical cantilever has been published [56]. In the next step the sensitivity has been driven even further. A nanocalorimeter [57] has been designed whose efficiency enables the thermal analysis of substances in the nano- and pico-gram range and with a picojoule sensitivity by using simple experimental equipment. The authors were able to quantify a solid-solid phase transition in n-alkanes in air. Only 7 pg of substance were needed which corresponds to a released heat of a mere 500 pJ. The calorimeter furthermore has a time resolution of only 0.5 ms, and dynamic effects can also be studied. Differences in the phase dynamics of odd and even-numbered n-alkanes were also studied.

An other example is shown in a publication [58] where samples in the nanogram range have been analyzed thermogravimetrically up to 300 ° C with piezo-resistive cantilevers.

This type of nanocalorimeter has also been applied to study nanoclusters, a large subfield of NSST. In a novel molecular beam experiment [59] the dependence of formation

energies of isolated Sn_N clusters on their size and shape has been investigated calorimetrically. The experimentally determined size dependence of the formation energy of Sn_N clusters consisting of between 95 and 97 atoms can be explained by the existence of two different types of neutral cluster isomers: One class of isomers is characterized by formation energies proportional to $N^{1/3}$, indicating compact spherical-like shapes. The other class has constant formation energies for the investigated size range, which is consistent with quasi-one-dimensional geometries. It would be of great interest to know more about the exact structure of this elongated clusters. How they might compare with or differ from carbon nanotubes.

5˙3. *A cantilever array-based artificial nose.* – The quantitative and qualitative detection of analyte vapors using a microfabricated silicon cantilever array (Fig. 18) is another example of nanomechanics. To observe transduction of physical and chemical processes

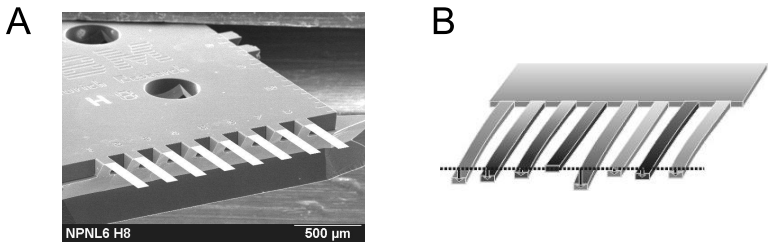

Figure 18. – (A) SEM image of a cantilever array. (B) Deflection signal relative to the *in situ* "reference" cantilever can be analyzed.

into nanomechanical motion of the cantilever, swelling of a polymer layer on the cantilever is monitored during exposure to analyte. (Mass take up could be an alternative, but needs a dynamic mode of operation.) This motion due to swelling is tracked by a beam-deflection technique using a time multiplexing scheme. The response pattern of eight cantilevers is analyzed *via* multivariate statistics and artificial neural network (ANN) techniques, which facilitate the application of the device as an artificial chemical nose. Analytes tested comprise chemical solvents, a homologous series of primary alcohols and natural flavors [60].

5˙4. *Translating Biomolecular Recognition into Nanomechanics.* – The single event molecular recognition experiments by mechanical response to external forces (see section 3.3) are very useful to get detailed insights into this process, however the technique might not be suitable for diagnostic applications. The focus in this section is on multiplying these effects and therefore increasing the sensitivity to make possible a more user friendly device.

A differential cantilever system [61] has been used to observe the specific transduction via surface stress changes of DNA hybridization and the molecular recognition between proteins into a direct nanomechanical response. Fig. 19 shows the scheme used illustrat-

ing the hybridization experiment. Each cantilever is functionalized on one side with a

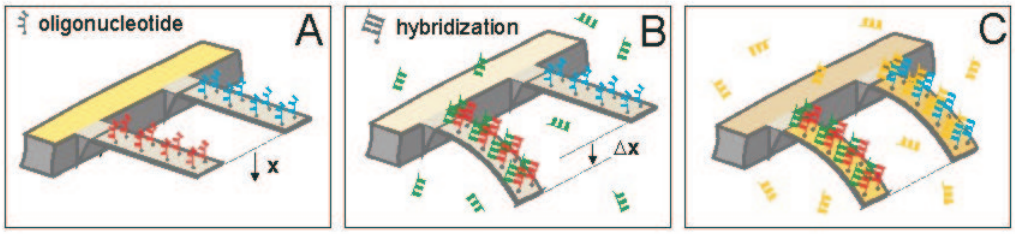

Figure 19. – Scheme illustrating the hybridization experiment. Each cantilever is functionalized on one side with a different oligonucleotide base sequence (red or blue). (A) The differential signal is set to zero. (B) After injection of the first complementary oligonucleotide (green), hybridization occurs on the cantilever that provides the matching sequence (red), increasing the differential signal Δx. (C) Injection of the second complementary oligonucleotide (yellow) causes the cantilever functionalized with the second oligonucleotide (blue) to bend [61].

different oligonucleotide base sequence (red or blue). A) The differential signal is set to zero. B) After injection of the first complementary oligonucleotide (green) hybridization occurs on the cantilever functionalized with the matching sequence (red), increasing the differential signal Δx. C) Injection of the second complementary oligonucleotide (yellow) causes the cantilever functionalized with the second oligonucleotide (blue) to bend. These experiments show that a single mismatch between two 12-mer oligonucleotides is clearly detectable. It is important to realize that in contrast to todays DNA sequencing experiments (e.g. Gene chips) these experiments have the advantage of working without markers and labels. Similar experiment on protein A $\leftrightarrow$ immunoglobulin interactions demonstrate the wide-ranging applicability of nanomechanical transduction to detect biomolecular recognition. The experiment was performed in a manner similar to the hybridization experiments except that one cantilever was covered with protein A and the other with bovine serum albumin (BSA) as a reference. A distinct differential signal was observed from rabbit IgG, but not from goat IgG, this reflects the known specific binding properties of protein A to IgG of different mammals.

Here, a possibility will be emphasized which is at the heart of NSST, nano makes nano. The nanoactuation mechanism has more wide-ranging implications. The forces of $\sim$1 nN involved, are sufficient to operate micromechanical valves and related microfluidic devices. This would permit the autonomous operation of micro- or nano-robotic machinery. Because the transduction eliminates the need of external power supplies and control systems, *in situ* delivery devices could be triggered directly by signals from single cells, gene expression, or immune responses.

5˙5. *MRFM, Millipede etc..* – An other promising application of the cantilever technique is the mechanical detection of NMR (see e.g. [62]). It is still an open question if the vision of single spin detection can be realized, but smaller mass detection and higher

spatial resolution compared to that obtained by conventional equipment will already be a breakthrough. A new industrial application of NSST might be the possible use of the millipede [63] for mechanical storage.

6. – Conclusions

It is the hope that newcomers to the field, Ph.D. students and others interested in the impact of SPM on NSST might enjoy the written version of the lectures as guidelines through a fascinating field that has developed over the past 20 years. To make this series of lectures most coherent, we have focused mainly on the activities in Switzerland.

SPM is an exciting novel experimental technique with a broad diversity. Initially it had a great impact on the local aspects of surface science. However, there was and is an innovative crew of scientists developing SPM more and more towards eyes and tools of NSST. These methods together with new nanoscale materials are the two fundamentals of the novel field of NSST. Since we are at the beginning of NSST, more exciting research results are expected to come and to create great fun among the science community.

* * *

First of all we would like to express our sincere thanks to the organizers of the Varenna Summer school. Second, we would like to thank our colleagues from Basel and Rüschlikon for the great collaborative effort and for their valuable contributions to make progress in the field of "Impact of SPM on NSST". We are greatful to Ernst Meyer, Christoph Gerber, Jim Gimzewski, Hans Hug, Mark Lantz, Roland Bennewitz, Hans-Peter Lang, Rolf Schäfer, Peter Vettiger and Wilfried Grange. We thank several generations of Ph.D. students and graduate students, in particularly our hard working technicians and all the people who contributed to this review.

Financial support is acknowledged from SNF, CTI, National Research Programs 24, 30, 36, Swiss Priority Program MINAST, Technology Oriented Program (TOP) NANO21 and the Treubel Foundation.

REFERENCES

[1] FEYNMAN, R.P., *Eng.Sci. Mag.* **23** (1960) 22.
[2] TANIGUCHI, N., *Proc. ICPE*, Tokyo (1974) JSPE
[3] International Technoloy Research Institute (1999) Loyola College in Maryland, Jan. 1999.
[4] FRENKEL, J., *J. Phys. Rev.* **36** (1930) 1604.
[5] BINNIG, G., ROHRER, H., GERBER, CH. and WEIBEL, E., *Phys. Rev. Lett.* **49** (1982) 57.
[6] GIAEVER, I., *Phys. Rev. Lett.* **5** (1960) 147.
[7] HANSMA, P.K., *Phys. Rep.* **30** (1977) 145.
[8] POHL, D.W, DENK, W. and LANZ, M., *Appl. Phys. Lett.* **44** (1984) 651.
[9] BINNIG, G., QUATE, C.F. and GERBER, CH., *Phys. Rev. Lett.* **56** (1986) 930.
[10] BINNIG. G., ROHRER, H., GERBER, CH. and WEIBEL, E., *Phys. Rev. Lett.* **50** (1982) 120.

[11] WIESENDANGER, R., TARRACH, G., BÜRGLER, D. and GÜNTHERODT, H.-J., *Europhys. Lett.* **12** (1990) 57.
[12] HAMERS, R., this volume no. 9.
[13] RINGER, M., HIDBER, H.R., SCHLÖGEL, R., OELHAFEN, P. and GÜNTHERODT, H.-J., *Appl. Phys. Lett.* **46** (1985) 832.
[14] STAUFER, U., WIESENDANGER, R., ENG. L., ROSENTHALER, L., HIDBER, H.R. and GÜNTHERODT, H.-J., *Appl. Phys. Lett.* **51** (1987) 244.
[15] STAUFER, U., SCANDELLA, L. and WIESENDANGER, R., *Z. Phys. B - Cond. Matt.* **77** (1989) 281.
[16] CROMMIE, M.F., LUTZ, C.P., EIGLER, D.M. and HELLER, E.J., *Surf. Rev. Lett.* **2** (1995) 127.
[17] MANOHARAN H.C., LUTZ, C.P. and EIGLER, D.M., *Nature* **403** (2000) 512.
[18] JUNG, T.A., SCHLITTLER, R.R., GIMZWESKI, J.K., TANG, C. and JOACHIM, C., *Science* **271** (1996) 181.
[19] GIMZWESKI, J.K. and JOACHIM, C., *Science* **283** (1999), 1683.
[20] JOACHIM, C., GIMZWESKI, J.K. and AVIRAM, A., *Nature* **408** (2000) 541.
[21] FISHLOCK, W., ORAL, A., EGDELL, R.G. and PETHICA, J.B., *Nature* **404** (2000) 743.
[22] HESS, H.F., ROBINSON, R.B., DYNES, R.C., VALLES, J.M. and WASZCZAK, J.V., *Phys. Rev. Lett.* **62** (1989) 214.
[23] BEHLER, S., PAN, S.H., JESS, P., BARATOFF, A. and GÜNTHERODT, H.-J., *Phys. Rev. Lett.* **72** (1994) 1750.
[24] PLOURDE, B.L. and VAN HARLINGEN, D.J., *Rev. Sci. Instrum.* **70** (1999) 4347.
[25] PAN, S.H., HUDSON, E.W. and DAVIS, J.C., *Rev. Sci. Instrum.* **70** (1999) 1459.
[26] STIPE, B.C., REZAEI, M.A. and HO, W., *Science* **280** (1998) 1732.
[27] GOLDSBURY, C.S., KISTLER, J., AEBI, U., ARVINTE, T. and COOPER, G.J.S., *J. Mol. Biol.* **285** (1999) 33.
[28] ENGEL, A. and MÜLLER, D.J., *Nature Struct. Biol.* **7** (2000) 715.
[29] HOWALD, L., LÜTHI, R., MEYER, E. and GÜNTHERODT, H.-J., *Phys. Rev. B* **51** (1995) 5484.
[30] MEYER, E., OVERNEY, R.M., DRANSFELD, K. and GYALOG, T., in *Nanoscience: Friction and Rheology on the Nanometer Scale*, (World Scientific Publishing) 1998
[31] GNECCO, E., BENNEWITZ, R., GYALOG, T., LOPPACHER, C., BAMMERLIN, M., MEYER, E. and GÜNTHERODT, H.-J., *Phys. Rev. Lett.* **84** (2000) 1172.
[32] FLORIN, E.L., MOY, V.T. and GAUB, H.E., *Science* **264** (1994) 415.
[33] MERKEL, R., NASSOY, P., LEUNG, A., RITCHIE, K. and EVANS, E., *Nature* **397** (1999) 50.
[34] STRUNZ, T., OROSZLAN, K., SCHÄFER, R. and GÜNTHERODT. H.-J., *Proc. Natl. Acad. Sci. USA* **96** (1999) 11277.
[35] DAMMER, U., POPESCU, O., WAGNER, P., ANSELMETTI, D., GÜNTHERODT, H.-J. and MISEVIC, G.N., *Science* **267** (1995) 1173.
[36] SCHWESIGNGER, F., ROS, R., STRUNZ, T., ANSELMETTI, D., GÜNTHERODT, H.J., HONEGGER, A., JERMUTUS, L., TIEFENAUER, L. and PLÜCKTHUN, A., *Proc. Natl. Acad. Sci. USA* **97** (2000) 9972.
[37] STRUNZ, T., OROSZLAN, K., SCHUMAKOVITCH, I., GÜNTHERODT, H.-J. and HEGNER, M., *Biophys. J.* **79** (2000) 1206.
[38] DE PARIS, R., STRUNZ, T., OROSZLAN, K., GÜNTHERODT, H.-J. and HEGNER, M., *Single Mol.* **1** (2000) 285.
[39] GIESSIBL, F.J., *Science* **267** (1995) 68.
[40] OHNESORGE, F. and BINNIG, G., *Science* **260** (1993) 1451.

[41] HOWALD, L., MEYER, E., LÜTHI, R., HAEFKE, H., OVERNEY, R., RUDIN, H. and GÜNTHERODT, H.-J., *Appl. Phys. Lett.* **63** (1993) 117.
[42] LÜTHI, R., MEYER, E., BAMMERLIN, M., BARATOFF, A., LEHMANN, T., HOWALD, L., GERBER, CH. and GÜNTHERODT, H.-J., *Z. Phys. B* **100** (1996) 165.
[43] LÜTHI, R., MEYER, E., BAMMERLIN, M., BARATOFF, A., HOWALD, L., GERBER, CH. and GÜNTHERODT, H.-J., *Surf. Rev. Lett.* **4** (1997) 1025.
[44] BENNEWITZ, R., FOSTER, A.S., KANTOROVICH, L.N., BAMMERLIN, M., LOPPACHER, CH., SCHÄR, S., GUGGISBERG, M., MEYER, E. and SHLUGER, A.L., *Phys. Rev. B* **62** (2000) 2074.
[45] LANTZ, M.A., HUG, H.J., VAN SCHENDEL, P.J.A., HOFFMANN, R., MARTIN, S., BARATOFF, A., ABDURIXIT, A., GÜNTHERODT, H.-J. and GERBER, CH., *Phys. Rev. Lett.* **84** (2000) 2642.
[46] VAN SCHENDEL, P.J.A., HUG, H.J., STIEFEL, B., MARTIN, S. and GÜNTHERODT, H.-J., *J. Appl. Phys.* **88** (2000) 435.
[47] HUG, H.J., SIEFEL, B., VAN SCHENDEL, P.J.A., MOSER, A., HOFER, R., MARTIN, S. and GÜNTHERODT, H.-J., *J. Appl. Phys.* **83** (1998) 5609.
[48] MOSER, A., HUG, H.J., PARASHIKOV, I., STIEFEL, B., FRITZ, O., BARATOFF, A., THOMAS, H., GÜNTHERODT, H.-J. and CHAUDHARI, P., *Phys. Rev. Lett.* **74** (1995) 1847.
[49] STIEFEL, B., HUG, H.J. et al., *unpublished results.*
[50] TSUEI, C.C., KIRTLEY, J.R., CHI, C.C., YUJAHNES, L.S., GUPTA, A., SHAW, T., SUN, J.Z. and KETCHEN, M.B., *Phys. Rev. Lett.* **73** (1994) 593.
[51] KIRTLEY, J.R., TSUEI, C.C., SUN, J.Z., CHI, C.C., YUJAHNES, L.S., GUPTA, A., RUPP, M. and KETCHEN, M.B., *Nature* **373** (1995) 225.
[52] CHANG, A.M., HALLEN, H.D., HARRIOTT, L., HESS, H.F., KAO, H.L., KWO, J., MILLER, R.E., WOLFE, R., VAN DER ZIEL, J. and CHANG, T.Y., *Appl. Phys. Lett.* **61** (1992) 1974.
[53] CHANG, A.M., HALLEN, H.D., HESS, H.F., KAO, H.L., KWO, J., SUDBO, A. and CHANG, T.Y., *Europhys. Lett.* **20** (1992) 645.
[54] GIMZWESKI, J.K., GERBER, CH., MEYER, E. and SCHLITTLER, R.R., *Chem. Phys. Lett.* **217** (1994) 589.
[55] BERGER, R., DELAMARCHE, E., LANG, H.P., GERBER, CH., GIMZEWSKI, J.K., MEYER, E. and GÜNTHERODT, H.-J., *Science* **276** (1997), 2021.
[56] BERGER, R., GERBER, CH., GIMZWESKI, J.K., MEYER, E. and GÜNTHERODT, H.-J., *Appl. Phys. Lett.* **69** (1996), 40.
[57] NAKAGAWA, Y. and SCHÄFER, R., *Angew. Chem. Int. Ed.* **38** (1999) 1083.
[58] BERGER, R., LANG, H.P., GERBER, CH., GIMZEWSKI, J.K., FABIAN, J.H., SCANDELLA, L., MEYER, E. and GÜNTHERODT, H.-J., *Chem. Phys. Lett.* **294** (1998) 363.
[59] BACHELS, T., SCHÄFER, R. and GÜNTHERODT, H.-J., *Phys. Rev. Lett.* **84** (2000) 4890.
[60] BALLER, M.K., LANG, H.P., FRITZ, J., GERBER, CH., GIMZWESKI, J.K., DRECHSLER, U., ROTHUIZEN, H., DESPONT, M., VETTIGER, P., BATTISTON, F.M., RAMSEYER, J.P., FORNARO, P., MEYER, E. and GÜNTEHRODT, H.-J., *Ultramicroscopy* **82** (2000) 1.
[61] FRITZ, J., BALLER, M.K., LANG, H.P., ROTHUIZEN, H., VETTIGER, P., MEYER, E., GÜNTHERODT, H.-J., GERBER, CH. and GIMZEWSKI, J.K., *Science* **288** (2000) 316.
[62] RUGAR, D., YANNONI, C.S. and SIDLES, J.A., *Nature* **360** (1992) 563.
[63] VETTIGER, P. this volume no. 14